

## Carbon and Oxygen Isotopic Systematics in Calcite and Dolomite from the Sangan Iron Skarn Deposit, Northeastern Iran

M. Boomeri,<sup>1,\*</sup> D. Ishiyama,<sup>2</sup> T. Mizuta,<sup>2</sup> O. Matsubaya,<sup>2</sup> and D.R. Lentz<sup>3</sup>

<sup>1</sup>Department of Geology, University of Sistan and Baluchestan, Zahedan, Islamic Republic of Iran

<sup>2</sup>Department of Earth Science and Technology, Akita University, Japan

<sup>3</sup>Department of Geology, University of New Brunswick, PO Box 4400, Fredericton, NB Canada E3B5A3

Received: 23 August 2009 / Revised: 19 May 2010 / Accepted: 5 June 2010

### Abstract

A total of 40 samples from carbonates and 8 samples from silicate rocks were analyzed from the Sangan iron skarn deposit to examine behavior of the oxygen and carbon isotopes. The higher values of  $\delta^{18}\text{O}$  are from metamorphic calcite and dolomite and lower ones are from granitic rocks. Although the  $\delta^{18}\text{O}$  and  $\delta^{13}\text{C}$  values of calcite and dolomite in marble yield the highest values in the Sangan deposit, they are still lower than those of normal marine limestone and dolomite, i.e., reflecting coupled decarbonation and infiltrative metasomatic effects. The  $\delta^{18}\text{O}$  and  $\delta^{13}\text{C}$  values of calcite from the Sangan deposit show a progressive, gradual depletion from least-altered marbles into proximal skarn. The gradual decrease of the  $\delta^{18}\text{O}$  and  $\delta^{13}\text{C}$  values from metamorphic calcite to skarn calcite and dolomite can be ascribed to interaction of hydrothermal fluids with carbonate rocks in the area with an increase of water to rock ratio. The isotopic mass-balance calculations suggest the presence of magmatic water in the Sangan deposit.

**Keywords:** Iran; Sangan; Iron skarn deposit; Stable isotopes

### Introduction

The Sangan iron skarn deposit is located about 300 km southeast of Mashhad, northeastern Iran. Although skarn deposits have been subjected of intensive studies in America, Japan, Europe, and some other countries and their characteristics are relatively well understood [27], there have been only a few studies on the Sangan skarn deposit and none of them include isotopic studies. Previous studies investigated some geological and economic aspects of the Sangan deposit [20, 21, 7, 5,

24, 8, 9, 10]. They have proposed several mineralization models for the Sangan deposit, such as magmatic segregation, volcano-sedimentary, and skarn types. The purpose of this study is mainly to determine the stable isotopic behaviour of O and C in carbonate minerals to discuss the nature of the fluids responsible for the formation of the dominante carbonate gangue minerals and the iron skarn deposit. Stable isotopes show variation of physical and chemical condition in natural geological environments. Isotopic data in combination with petrographic and petrological studies allow to

\* Corresponding author, Tel.: +98(541)2417890, Fax: +98(541)2446565, E-mail: boomeri@hamoon.usb.ac.ir

deduce the sources and compositions of ore-bearing fluids and wall rock-water interaction for the Sangam ore deposit and related igneous rocks.

Carbon and oxygen isotope studies of calcite and dolomite in contact-metamorphic aureoles and skarn deposits have already been proved useful to interpret their genesis [3, 11, 12, 13, 14, 18, 28, 29, 33, 35, 38, 39, 43, 49, 50, 52]. These studies have demonstrated that calcite and dolomite in contact-metamorphic aureoles and skarn deposits are mainly formed by magmatic water. Therefore, the skarn calcite and dolomite can be used as a good tracer of magmatic water in ore mineralization fields.

### Geological Setting

Iran is geologically divided into many structural zones with different characteristics (Fig. 1). All these zones were formed by the opening and closing of Paleo- and Neotethys oceanic basins due to subduction and collision events in south and north of Iran. The north side of Iran collided with Turkmenistan or Turan plate (Eurasia) in late Triassic-early Jurassic period [4]. To the south Iran was subducted and collided by Arabian plate starting from Late Cretaceous [4] and continuing into the Miocene and later times [1, 51].

The Sangam iron deposit is located in Central Iran zone. In this zone, igneous activity starting in the Eocene period (50 Ma) and reaching to its highest point during the middle Eocene for exposed volcanic rocks and Oligo-Miocene for plutonic rocks in many parts of Iran [4]. These types of volcanic and plutonic rocks are generally associated with extensive porphyry copper mineralization in the Central Iran zone, such as at Sungun [19], Sarchesmeh, Miduk, and many other subeconomical ore bodies.

The study area is located in regional geological maps (1:100000 scale) of Taybad [48] and Khaf [2] areas. Most of the rock units are part of a NW-SE trending mountain range named as the Main range [48]. Although the oldest sedimentary rocks in the Sangam mining area were attributed to late Proterozoic [48], recent studies show that the oldest unit in the Sangam district are lower Jurassic metamorphosed shale, siltstone, and sandstone [8] (Fig. 2). This unit is overlain by Middle to Upper Cretaceous limestone and dolomite, which toward to the south are unconformably overlain by thick sequence of Eocene volcanoclastic and pyroclastic rocks interlayered with lava (Fig. 2). The volcanic rocks are mainly andesite, dacite, and rhyolite.

These units are intruded by a W-E elongate late Eocene-early Oligocene granitic batholith, named the Sarnowsar and Sarkhar granitoids, and many syn- and

post-mineralization felsic stocks and dykes in the Sangam area (Fig. 2). The Sarnowsar batholith-sized granitoid mass is mainly located on north side of the mineralization zone. The granitoid ranges from alkali granite to granodiorite (Fig. 3) with granular and porphyritic textures. They are mainly composed of quartz, K-feldspar, plagioclase, biotite, amphibole, titanite, magnetite, apatite, and zircon. The pluton has metaluminous I-type characteristics and has high content of alkalis ( $\text{Na}_2\text{O} + \text{K}_2\text{O} > 8 \text{ wt } \%$ ) and high concentration of light REE. The felsic dykes are dacitic to alkaline rhyolitic in composition with porphyritic texture. It is difficult to discriminate dykes as premineral, intramineral or post-mineralization, because the mineralization is lithologically controlled by carbonate rocks. Some felsic dykes that are associated with mineralization are potassic-rich and their  $\text{K}_2\text{O}$  is more than 7 wt %. The Sangam granitic rocks evidently formed from partial melting of metasomatized mantle-derived rocks, which were contaminated by arc-like crustal materials [8], in a convergent margin setting. The country rocks are contact metamorphosed and extensively metasomatized around the granitoid batholith. The granitoid-related metamorphism produced quartzite and biotite-feldspar hornfels in the sandstone and shale and olivine-pyroxene grade marble in the carbonate rocks. The contact metamorphic aureole is locally overprinted by hydrothermal processes, which resulted in sericitization, carbonatization, silicification, chloritization, and K-feldspar alteration scattered in non-carbonate rocks and skarnification in the carbonate rocks [8].

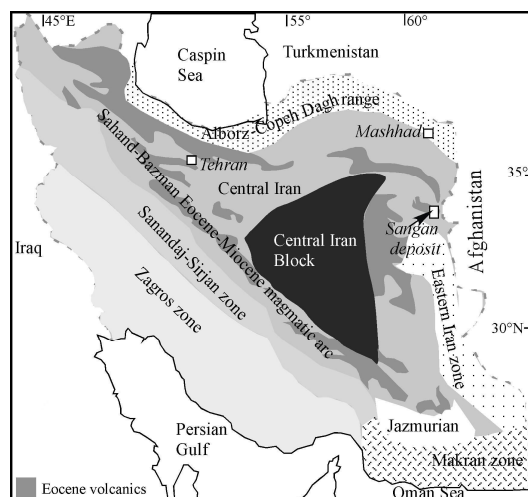


**Figure 1.** Generalized geological map showing the major structural zones of Iran and the distribution of volcanic and plutonic rocks [4, 40].

### Ore Mineralization

Numerous iron ore bodies occur in the Sangan area named as Western, Middle, and Eastern ore bodies (Fig. 2). The most important is the Western ore deposit, which is located mainly in the southern part of the Sarnowsar granitoid (Fig. 2-b). The Sangan iron ores and skarns were mainly formed within the carbonate rocks, which extend along the strike of the granitic batholith (Fig. 2). The ores occur as stratabound massive ores, and sometimes as disseminated and crosscutting vein and veinlets. The carbonate host rocks are mainly away from the granitoid border (some more than 1 km away). However, some iron ore bodies and intensive skarn zones are in contact with the main batholith. Based on the host rocks, mineralogy, and whole-rock composition, the Western ore deposit can be divided into two distinct skarn zones: 1-calcic skarn zone and 2- magnesian skarn zone (Fig. 2).

The calcic skarn zone extends about 4.5 km with a trend of SSE. Northwest of this zone is in contact to the Sarnowsar granitoid and intruded by a swarm of potassic rhyodacitic and dacitic dykes and granitic apophyses (Fig. 2). The calcic skarn zone replaced calcite marble and can be subdivided into garnet-magnetite and carbonate-magnetite zones (Fig. 2). The garnet-magnetite zone occupies both western and eastern extent of the calcic skarn zone where it was completely replaced by skarns and magnetite ores. To the northwest of the calcic zone, volcanic and pyroclastic rocks were also replaced by salite and marialitic scapolite. Prograde skarn mineralogy in the garnet-magnetite zone consists dominantly of grossular-andradite solid solution series and hedenbergitic clinopyroxene. The retrograde skarn mineralogy consists of dominantly early hastingsite and later actinolite, chlorite, analcime, and euhedral calcite. Magnetite ores are small and low grade in this zone.

Although, the carbonate-magnetite zone is located about 1 km away from the Sarnowsar granitoid border, high-grade thick massive magnetite ores replaced marble and limestone directly in this zone rather than replacing an earlier skarn. The silicate minerals consist of a few (10 %) diopsidic clinopyroxene and tremolite in non-mineralized marbles in this zone. In fact, the calc-silicates those are typical of skarns, such as garnet, are virtually absent from the carbonate-magnetite zone. Calcites occur as long lenses and veins and pure euhedral crystals in this zone. The marbles and magnetite ores are surrounded by Eocene rhyolitic volcanic rocks in carbonate-magnetite zone. The rhyolitic rocks are extensively altered and veined to calcite and quartz and they show rhythmic and

concentric iron oxide-contaminated layer, which was produced by weathering. The felsic intrusions in this zone are non-mineralized and extensively altered to calcite and sericite.

The magnesian skarn zone replaced thick dolomitic marble and elongated in a NW-SE direction with a length more than two km. Magnetite ores are mainly high-grade, massive thick layers that are surrounded by dolomitic marbles in this zone. Low-grade marbles in this zone contain a few percent skarns minerals. The prograde skarn mineralogy is dominated by forsterite, diopside, and phlogopite in the magnesian skarn zone. The retrograde mineralogy consists dominantly of

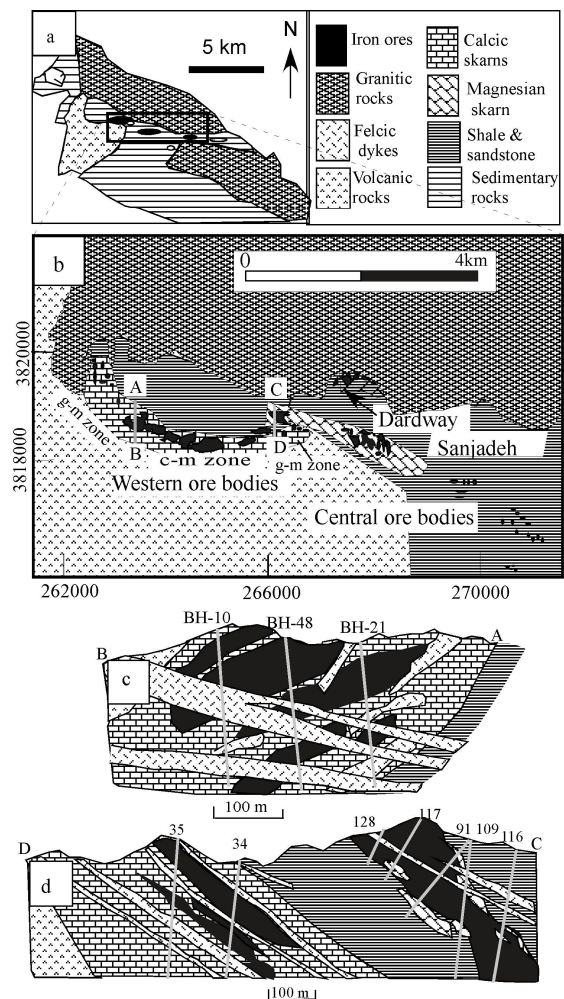


**Figure 2.** Simplified geological maps (a and b) showing distribution of the iron ores in the Sangan deposit. c) a N-S cross section from g-m zone, d) a N-S cross section from magnesian zone ( north side) and g-m zone (south side). g-m = garnet-magnetite and c-m = carbonate-magnetite, BH = borehole.

tremolite, clinocllore, and serpentine. This zone is also located away from Sarnowsar granitoid, but it intruded by several potassic felsic dykes. The felsic dykes locally were altered to calcite and clay minerals in this zone.

Opaque minerals are similar throughout the ore deposit mainly composed of major magnetite and minor chalcocopyrite, pyrrhotite, pyrite, and hematite [8].

Like many skarn deposits [15, 26], the Sangan Iron deposit was formed during two main stages [8]; the early contact metamorphic stage is overprinted by a later metasomatic stage, of which the metasomatic stage is subdivided into prograde and retrograde substages. Weathering also formed many minerals such as goethite, limonite, martite, Cu carbonates, and native copper [8]. The mineral assemblages in the Sangan deposit (e.g., absence of wollastonite) indicate that the metasomatic stage developed below 520°C [8].

### Carbonate Minerals

Calcite is a common mineral both in the magnesian and the calcic zone, but dolomite is more common in the magnesian zone. Other carbonate minerals are siderite and ankerite, which locally occur in the carbonate-magnetite zone. The carbonates in the Sangan ore deposits can be divided into 5 types as follows:

I) Metamorphic type: This type includes calcite and dolomite marbles and recrystallized limestone and dolomite. Calcite marble and limestone are host rocks in the calcic zone and were partly replaced by magnetite and skarn minerals. Non-mineralized marbles are composed mainly of calcite and small amounts of pyroxene, tourmaline, and amphibole. Dolomite marble is the main part of the magnesian zone and was locally replaced by iron oxides. Non-mineralized dolomitic marble is mainly composed of dolomite, calcite, and small amounts of olivine, serpentine, and phlogopite.

II) Skarn type: Interstitial calcite and dolomite in skarn minerals are considered as skarn type, including skarn calcite and skarn dolomite. Petrographic studies show that the skarn type was formed due to the breakdown of early calc-silicates, such as garnet and clinopyroxene and the replacement of magnetite in skarns and carbonate rocks by hydrothermal solutions. The skarn calcite occurs in both the calcic skarn and the magnesian skarn zones. The skarn dolomite occurs in the magnesian zone and is commonly interstitial in phlogopite and magnetite intergrowths.

III) Weathering type: Late calcite and dolomite veins have a banded structure and occupy fractures and open spaces cutting all other mineral assemblages. Late dolomite veins occur in the magnesian zone, whereas late vein calcites occur in the carbonate-magnetite zone.

The early carbonate sometimes dissolve by surface waters and migrated a long fractures then again formed as new precipitates.

IV) Calcite that replaced plagioclase crystals in the felsic dykes (calcite in felsic dykes).

V) Calcite in limestone from Khajeh Anjireh is considered fresh limestone and used for comparison with their data from altered marbles in the Sangan deposit. This limestone is about 10 km away from the Sangan ore deposit toward the south.

### Fluid Inclusions

The skarn calcite in the Sangan deposit hosts two, three, and rarely four phase and high salinity fluid inclusions (Fig. 4). The vapour phase in the fluid inclusions disappeared ( $T_h$ ) in the range of 100 to 121°C and 193 to 217°C (Table 1). Dissolution of daughter minerals (typically halite) in the three phase fluid inclusions from skarn calcite occurred in the range of 140 to 150°C and 230 to 245°C (Table 1). Salinities of the fluid inclusions in the calcite range from 18.24 to 34.4 wt % equivalent NaCl (Table 1). The daughter minerals homogenize after vapour bubbles, indicating the pressure is relatively high. Similar temperatures and salinity were reported for fluid inclusions in the skarn

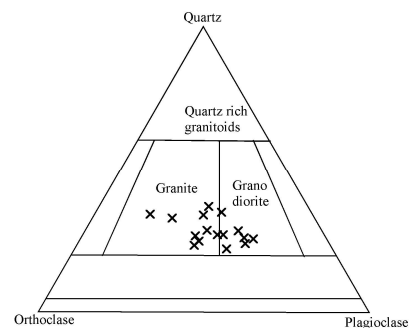


**Figure 3.** Ternary plots of the modal quartz, plagioclase, and orthoclase of the Zahedan granitic rocks. The fields from [41].

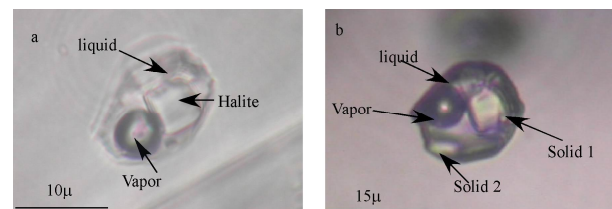


**Figure 4.** Photomicrograph of fluid inclusions in skarn calcite from the Sangan deposit. (a) Three phase fluid inclusion, (b) Four phase fluid inclusion.

calcite from the Neuquen skarn and porphyry deposits [16]. With pressure correction, trapping temperatures ( $T_t$ ) for the skarn calcite are higher. Therefore, the fluids circulated in the calcite skarn show two ranges of homogenization temperature, low- and high-T types. The low-T type occurs in the magnetite-carbonate zone and high-T type occurs in garnet-magnetite zone. Although fluid inclusions in calcite are not ideally suitable for thermometry, the homogenization temperatures are consistent with calcite skarn formation, which is a late mineral in skarn systems and form at temperatures less than 300°C.

Quartz in the Sarnowsar granitoid contains several generations of fluid inclusions. The fluid inclusions in the granite are two-phase fluid inclusions associated with polyphase and vapour-rich inclusions. Salinity of these fluid inclusions ranges from 30 to 70 wt. % equivalent NaCl [8]. The homogenization temperatures range from 200 to 550°C. The fluid inclusions in pegmatitic quartz veins close to the Sarnowsar granitoid border also show a wide range of homogenization temperatures for circulated fluids averaging 500°C. The fluid inclusions in the quartz have characteristics of those of which were described for porphyry and skarn deposits by [34] and probably were formed by magmatic waters exsolved from the Sarnowsar granitoid melts during emplacement.

### Sampling and Analytical Methods

#### Carbonates

A total of 40 pure calcite and dolomite samples from all zones of the ore deposit were analyzed for oxygen and carbon isotopes. These samples were examined by X-ray diffraction and some of them petrographically. Descriptions of the samples from different carbonate types in the Sangan ore deposits are given in Table 2. About 20 mg of powdered carbonate were decomposed in 100 % phosphoric acid at 25°C following the method of [25] to obtain carbon dioxide gas for isotopic analyses. The time for calcite samples to decompose was one day, whereas dolomite samples took about one month to decompose completely. The released CO<sub>2</sub> gas was collected in a liquid N<sub>2</sub> trap. Then, the CO<sub>2</sub> gas was separated from water vapour by the substitution of a dry-ice-acetone trap. Isotopic measurements of the CO<sub>2</sub> gas were carried out using a Finnigan MAT 250 Mass Spectrometer of Akita University. All data are given in terms of a conventional  $\delta$  expression in per mil unit relative to PDB for carbon isotopic ratio and SMOW for oxygen isotopic ratio. The analytical reproducibility is  $\pm 0.1$  per mil for carbon and  $\pm 0.3$  per mil for oxygen.

#### Silicates

The following whole-rock samples from the silicate country rocks were analyzed for oxygen isotopes: Four samples from the Sarnowsar granite, one sample from the dacite porphyry, one sample from the hornfels in the garnet-magnetite zone, one sample from the felsic dyke in the garnet-magnetite zone and one sample is pure euhedral quartz from the carbonate-magnetite zone (BH-57). Description of these samples is given in Table 3. About 20 mg of powdered sample from aluminosilicate rocks are reacted in F<sub>2</sub> gas, a technique described by [22], in a nickel tube at 500°C for twelve hours to produce O<sub>2</sub> gas. The gas was then converted to CO<sub>2</sub> gas in a graphite furnace at 700°C and collected by a Toeple pump and liquid nitrogen trap.

## Results and Discussion

#### Silicates

$\delta^{18}\text{O}$  values of country rocks including Sarnowsar granite from the Sangan area given in Table 3. The  $\delta^{18}\text{O}$  values of whole-rock samples from the granitoid range from 9.5 to 8.9 ‰. The  $\delta^{18}\text{O}$  value of one sample from plug-like granite porphyry is 9.5 ‰ (apophyses of the main pluton in the garnet-magnetite zone). Variation in

**Table 1.** Representative microthermometry data of two phase and three phase fluid inclusions in skarn calcite from the Sangan deposit

Samples	Phases	$T_h$ vapor	$T_{fm}$	$T_h$ halite	Salinity
21131	2	319	-26.3	-	26.38
21132	2	109	-26.3	-	26.38
2112	2	104	-26.4	-	26.44
2113	2	101	-27.6	-	27.18
2115	2	103	-25.6	-	25.92
21136	2	119	-14.5	-	18.24
211311	2	121	-22	-	23.71
211312	3	114	-	142	29.3
211313	3	118	-	151	29.7
DG39	3	105	-	134	29.1
DG31	3	202	-	230	33.5
DG33	3	217	-	230	33.5
DG37	3	202	-	245	34.4

Note: Salinity is approximately estimated for the binary system NaCl-H<sub>2</sub>O in terms of eq. wt % NaCl.  $T_h$ = Temperature of homogenization,  $T_{fm}$ = Temperature of final melting. The salinity was calculated from the equations of Bodnar and Vityk (1994).

**Table 2.**  $\delta^{18}\text{O}$  and  $\delta^{13}\text{C}$  values of the calcite and dolomite from the Sangan Iron deposit

Samples	Type	Sample description	$\delta^{18}\text{O}$ (‰ SMOW)	$\delta^{13}\text{C}$ (‰ SMOW)
969M	Type I	A altered marble <sup>CM</sup>	12.4	-0.9
GB9	Type I	A gray marble <sup>CM</sup>	12.9	1.5
96-2	Type I	A ankeritic marble <sup>CM</sup>	20.9	-0.8
N1	Type I	Marble <sup>CM</sup>	14.9	1.2
N2	Type I	Marble <sup>CM</sup>	14.5	-0.3
21-14	Type I	Marble <sup>CM</sup>	15.9	-7.4
A'4	Type I	Marble <sup>CM</sup>	14.2	0.1
NC2D	Type I	Dolomite marble <sup>M</sup>	18.3	-0.8
223D	Type I	Dolomite marble <sup>M</sup>	25.5	0
214106D	Type I	Dolomite marble <sup>M</sup>	15.7	-0.2
96-2	Type I	Ankeritic marble <sup>CM</sup>	27.5	1.1
223-0	Type I	Dolomite marble <sup>M</sup>	22.6	-0.9
214-106	Type I	Dolomite marble <sup>M</sup>	15.5	-0.3
NC2	Type I	Dolomite marble <sup>M</sup>	15.6	-1.6
21--1	Type II	Interstitial calcite in ga <sup>GM</sup>	12.3	-5.8
969C	Type II	Interstitial calcite in marble <sup>CM</sup>	12.8	-1.7
57-12	Type II	Calcite vein with quartz <sup>CM</sup>	10.3	-2.4
21-23	Type II	Calcite vein <sup>A'</sup>	11.9	-2
21-13	Type II	Interstitial calcite in ga <sup>GM</sup>	11.3	-5.4
21--10	Type II	Interstitial calcite in magnetite ore <sup>GM</sup>	11.7	-5.4
A'3	Type II	Interstitial calcite in garnet skarn <sup>GM</sup>	11.3	-5.7
96-11	Type II	Interstitial calcite in magnetite ore <sup>CM</sup>	11.3	-2.6
BS10	Type II	Calcite vein <sup>CM</sup>	10.9	-2.6
57-7	Type II	Calcite vein with qz <sup>CM</sup>	10.2	-2.1
A'2	Type II	Interstitial calcite in garnet skarn <sup>GM</sup>	10.9	-4.8
96-8	Type II	Interstitial calcite in magnetite ore <sup>CM</sup>	11.4	-2.6
South C	Type II	Interstitial calcite in garnet skarn <sup>GM</sup>	11.2	-5.6
BK1	Type II	Interstitial dolomite in phlogopite skarn <sup>M</sup>	13.7	-0.9
917D	Type II	Interstitial dolomite in phlogopite skarn <sup>M</sup>	13.6	-2.1
57-8	Type II	A altered marble <sup>CM</sup>	10.3	-3
91-10	Type II	Interstitial calcite in phlogopite skarn <sup>M</sup>	9.9	-3.1
91-7	Type II	Interstitial calcite in phlogopite skarn <sup>M</sup>	12.4	-2.4
SB6	Type III	Late calcite vein <sup>CM</sup>	21.5	-0.2
NCC	Type III	Late calcite vein <sup>M</sup>	18	-5.4
NC3L	Type III	Late dolomite vein <sup>M</sup>	18.1	-5.5
NC3S	Type III	Late dolomite vein <sup>M</sup>	16.6	-5.9
NCD	Type III	Late dolomite vein <sup>M</sup>	17.6	-5.9
NC1	Type IV	Calcite in altered dacite <sup>M</sup>	22.5	-7.5
KHA1	Type V	Silicic limestone <sup>KA</sup>	19.5	0.7
KHA2	Type V	Silicic limestone <sup>KA</sup>	17.6	0.7

Note: CM = Carbonate-magnetite zone, GM = Garnet-magnetite zone M = Magnesian zone.

$\delta^{18}\text{O}$  values of these samples is less than 1.0 ‰. The very close similarity in  $\delta^{18}\text{O}$  values of the samples and sample range are consistent with equilibrium with a homogeneous fluid (e.g., silicate magma). The  $\delta^{18}\text{O}$  values of whole rock from the Sangan granitic rocks are slightly higher than for typical I-type granitoids (from +6.0 to +8.0 ‰, [47]). The higher  $\delta^{18}\text{O}$  values may be indicating crustal contribution to the magma or direct exchange between the granitic melt and the metasedimentary rocks [47]. However, there is also a good possibility that the higher  $\delta^{18}\text{O}$  values of the Sarnowsar granitoid and plug-like granite porphyry were produced by sub-solidus processes, such as deuteric and hydrothermal effects or low temperature hydration and weathering. For granite,  $\Delta^{18}\text{O}_{\text{whole rock-water}}$  is close to  $\Delta^{18}\text{O}_{\text{plagioclase-water}}$  [46]. Therefore, the  $\delta^{18}\text{O}$  value of a fluid in equilibrium with the Sangan granitic rocks can be calculated in temperature of 550° C (based on the fluid inclusion in granitoid and pegmatitic quartz vein) and the oxygen isotopic fractionation factor of Anorthite<sub>30</sub>-water ( $1000\ln\alpha_{\text{An-H}_2\text{O}}=2.68(10^6/T^2)-3.29$  from [32]). The  $\delta^{18}\text{O}$  value calculated for this fluid ranges from 9.2 to 8.6 ‰ with an average of 9.0 ‰ (Table 3).

The  $\delta^{18}\text{O}$  values of a felsic dyke is 11.9 ‰ (Table 3), which has  $\delta^{18}\text{O}$  values about 3.0 per mil higher than those of the main pluton on average. On the other hand a metasediment sample (metamorphosed shale or hornfels) from adjacent to the dyke has  $\delta^{18}\text{O}$  value of 13.1‰. Higher values of the felsic dykes could in part be due to the exchange effects with the metasediments. The magmatic hydrothermal fluids at relatively low temperatures could also increase  $\delta^{18}\text{O}$  value of the felsic dykes [47].  $\delta^{18}\text{O}$  value of pure quartz from a calcite-quartz vein is 12.9 ‰. This value falls in range of hydrothermal quartz veins.

### Carbonates

$\delta^{18}\text{O}$  and  $\delta^{13}\text{C}$  values of calcite and dolomite from the Sangan deposit are presented in Table 2 and are plotted in Figures 5 and 6. The  $\delta^{18}\text{O}$  values of calcite in calcite marble range from 12.4 to 14.9 ‰ and  $\delta^{13}\text{C}$  from -0.3 to 1.5 ‰. The  $\delta^{18}\text{O}$  values of calcite in dolomitic marble vary from 15.6 to 22.6 ‰ and  $\delta^{13}\text{C}$  from -1.6 to -0.3 ‰. The  $\delta^{18}\text{O}$  values of dolomite in dolomitic marble range from 15.7 to 25.5 ‰ and  $\delta^{13}\text{C}$  from -0.8 to 0.0 ‰. The  $\delta^{18}\text{O}$  and  $\delta^{13}\text{C}$  values of skarn calcite range from 9.9 to 12.8 ‰ and -1.7 to -5.8 ‰, respectively. The  $\delta^{18}\text{O}$  and  $\delta^{13}\text{C}$  values of skarn dolomite range from 13.6 to 13.7 ‰ and from -2.1 to -0.9 ‰, respectively.

The majority of samples from calcite marbles are strongly depleted in  $\delta^{18}\text{O}$  relative to normal marbles and

limestones of Cretaceous age (Fig. 5). Calcite and dolomite in samples from the dolomite marble also show depletion of  $\delta^{18}\text{O}$  (Fig. 6).  $\delta^{18}\text{O}$  and  $\delta^{13}\text{C}$  values of limestone from the Khageh Anjireh (as fresh samples) are also slightly lower than those of Cretaceous limestones. Original limestones in the area probably had higher  $\delta^{18}\text{O}$  and  $\delta^{13}\text{C}$  values. The  $\delta^{18}\text{O}$  and  $\delta^{13}\text{C}$  values of carbonates are sensitive to decarbonation, infiltration, and temperature [50]. Decarbonation processes can in some cases explain isotopic variations during contact

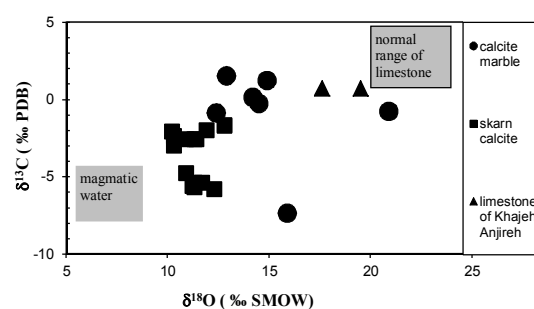


**Figure 5.**  $\delta^{18}\text{O}$  (SMOW) versus  $\delta^{13}\text{C}$  (PDB) of calcite from the calcic skarn zone. The isotopic values lie between those of normal limestone [50] and normal magmatic water [45].

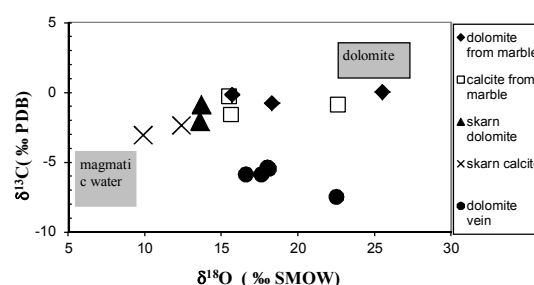


**Figure 6.** The  $\delta^{18}\text{O}$  and  $\delta^{13}\text{C}$  of calcite and dolomite from the magnesian skarn zone. The isotopic values lie between those of normal dolomite [42] and normal magmatic water [45].

**Table 3.**  $\delta^{18}\text{O}$  values of silicate rocks and minerals from the Sangan deposit

Samples	Rock types	$\delta^{18}\text{O}$ (‰ SMOW)	$\delta^{18}\text{O}$ (‰ SMOW)
G1 A	Granite	9.5	9.2
DG1	Granite	9.5	9.2
SG3	Granite	9	8.7
G7	Granite	8.9	8.6
A"2	Dacite	9.5	9.2
A'6	Hornfels	13.1	
21-24	Altered dacite	11.9	
57-12	Quartz	12.9	

metamorphism [11, 23, 39, 43]. [50] modeled effects of devolatilization and decarbonation with two end member processes: 1) Batch devolatilization where all fluids are evolved before any is permitted to escape (a closed system) and 2) Rayleigh devolatilization where each volatile molecule is immediately isolated from its rock of origin due to steady and perhaps slow expulsion (an open system). Magnitude of volatilization effects are shown by [50] through:  $\delta_f = \delta_i - (1-F)1000\ln\alpha$  for Batch devolatilization and  $\delta_f = 1000(F^{\alpha-1} - 1) + \delta_i$  for Rayleigh devolatilization. Where F is the mole fraction of the element of interest that remains in the rock after devolatilization,  $\alpha$  is the fractionation factor (fluid-Rock) and  $\delta_i$  and  $\delta_f$  are the initial and final isotopic values of the rock. Many published studies have reported  $^{18}\text{O}$  and  $^{13}\text{C}$  depletions in metamorphic aureoles involving carbonate rocks [11, 30, 36, 39, 43, 50]. They indicated that the effect of decarbonation reactions on  $\delta^{18}\text{O}$  depletions in carbonate rocks is always small, a few per mil, because the mole fraction of oxygen is considerable ( $F > 0.6$ ) even if decarbonation is complete. The effect of decarbonation on  $\delta^{13}\text{C}$  values may be much larger because in contrast to  $\delta^{18}\text{O}$ , F can be low as 0. The process of  $\delta^{18}\text{O}$  and  $\delta^{13}\text{C}$  depletions due to Batch and Rayleigh devolatilization was also calculated in this study for the calcite marbles, based on the above equations. For oxygen, we used the fractionation equation:  $1000\ln_{\text{CO}_2\text{-Calcite}} = -1.8(10^6/T^2) + 10.611(1000/T) - 2.78$  [17]. For carbon, we used the fractionation equation:  $1000\ln_{\text{calcite-CO}_2} = 2.988(10^6/T^2) - 7.66(1000/T) + 2.46$  [17]. Regarding the  $\delta^{18}\text{O}$  and  $\delta^{13}\text{C}$  values of calcite from the Khageh Anjireh as fresh limestones,  $\delta^{18}\text{O}$  and  $\delta^{13}\text{C}$  values of 20.0 and 1.0 ‰, respectively, were chosen as the starting point of the calculations assuming a maximum temperature of 520°C determined from the mineral assemblages [8] and a minimum temperature of 300°C. The mole fraction of oxygen remaining in the rock ( $F^{\text{O}}$ ) is assumed  $> 0.6$ , because  $F = 0.6$  is limit calc-silicates [50] when all carbonates are replaced by calc-silicates and the mole fraction of carbon remaining in the rock ( $F^{\text{C}}$ ) is zero. In the Sangam area, replaced calc-silicates such as diopside, olivine, amphibole, and mica in non-mineralized marble are seldom more than 10%. Using  $\alpha^{13}\text{C}$  ( $\text{CO}_2\text{-rock}$ ) and  $\alpha^{18}\text{O}$  ( $\text{CO}_2\text{-rock}$ ) at a temperature of 520°C,  $\delta_i^{18}\text{O} = 20$  ‰ and  $\delta_i^{13}\text{C} = 1$  ‰, the contents of  $\delta^{18}\text{O}$  and  $\delta^{13}\text{C}$  depletion was calculated both for Batch and Rayleigh processes. Neither Batch nor Rayleigh decarbonation is sufficient to explain the large  $\delta^{18}\text{O}$  depletion of the marble calcite and some of the dolomite marbles (Fig. 7). Even if all of the calcite reacts out of the system ( $F^{\text{O}}=0.6$ ), the calculated  $\delta^{18}\text{O}$  depletions are small and the calculated  $\delta^{18}\text{O}$  and  $\delta^{13}\text{C}$  do not coincide with those

of the study area (Fig. 7). The calculations in this study shows that the isotopic shifts in  $\delta^{18}\text{O}$  and  $\delta^{13}\text{C}$  values of calcite and dolomite from the Sangam deposits can not be explained only by simple volatilization.

Sample number 969M is a calcite marble cut by a skarn calcite vein (sample number 969C, Table 2). Although these two samples are different in occurrence and texture, their  $\delta^{18}\text{O}$  and  $\delta^{13}\text{C}$  values are similar. A quartz-actinolite-bearing marble (sample 57-8, Table 2) is strongly depleted in  $\delta^{18}\text{O}$  and  $\delta^{13}\text{C}$ . The sampling location of this sample is from the same borehole as samples 57-12 and 57-7. Although these samples are different in texture and formation, they are similar in isotopic values (Table 2). The metamorphic calcites and the skarn calcites with similar and lower values of  $\delta^{18}\text{O}$  and  $\delta^{13}\text{C}$  suggest an isotopic homogenization due to a locally more extensive fluid flow from the skarn zones, because of a higher permeability in fractured and brecciated zones. Another isotopic anomaly is the low  $\delta^{13}\text{C}$  values in marble sample 21-14 that is cut by veinlets of calcite, magnetite, and pyrite (Table 2). These values are similar to those of the late calcite and dolomite veins and calcite from the altered igneous rocks. Such isotopic values can be explained by infiltration of low temperature fluids. Formation of calcite and pyrite veins in marble sample 21-14 could also be due to these low temperature fluids ( $< 300^\circ\text{C}$ ).

The  $\delta^{18}\text{O}$  and  $\delta^{13}\text{C}$  values of calcite and dolomite in the magnesian zone show a systematic variation with

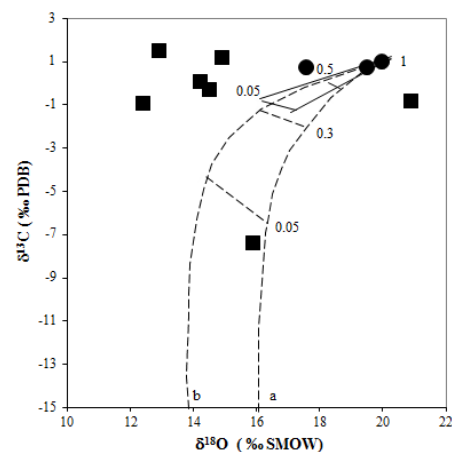


**Figure 7.** Plot of  $\delta^{18}\text{O}$  versus  $\delta^{13}\text{C}$  calculated from batch (solid straight lines) and Rayleigh (dashed curve lines) decarbonation. Assuming normal calc-silicate decarbonation,  $\delta^{18}\text{O}_i = +20.0$  ‰ and  $\delta^{13}\text{C}_i = +1.0$  ‰ at temperatures of 520°C (a) and 300°C (b). The lines are graduated in increments of  $F^{\text{C}}$  (mole fraction of C that remains in the rock). The filled squares are isotopic values of calcite marble from the Sangam deposit and limestone from the Khageh Anjireh.

degree of alteration. Sample 223D (Table 2) is an olivine-bearing dolomite marble, which also contains calcite. The olivine in this sample is less affected by alteration. However, it clearly shows that hydrothermal fluids traveled along microfractures and grain boundaries and some of the calcites and dolomites are products of reactions between host rock and fluids. This sample, which is the least altered sample, has the highest  $\delta^{18}\text{O}$  and  $\delta^{13}\text{C}$  values in the magnesian zone. In contrast, samples 214-106 and NC2 are more strongly depleted in  $\delta^{18}\text{O}$  than sample 223D (Table 2). Olivine and carbonates in these samples are partly replaced by magnetite  $\pm$  chalcopyrite, pyrite and sphalerite, olivine is strongly serpentinized. There is a strong evidence of a positive correlation between depletion of  $\delta^{18}\text{O}$  and  $\delta^{13}\text{C}$  and alteration grade and ore mineralization.

The skarn calcites and dolomites are characterized by a narrow range of  $\delta^{18}\text{O}$  values, while the  $\delta^{13}\text{C}$  values vary strongly. The  $\delta^{13}\text{C}$  of skarn calcite in the garnet-magnetite zone ( $\delta^{13}\text{C} = -4.8$  to  $-5.7$  ‰) are lower than those of skarn calcite in the carbonate-magnetite zone ( $\delta^{13}\text{C} = -3.0$  to  $-1.7$  ‰) and generally the  $\delta^{13}\text{C}$  of skarn calcites in the Sangam deposit are higher than those of magmatic fluids and must be affected by the  $\delta^{13}\text{C}$  of host marble. Variation in  $\delta^{13}\text{C}$  values are usually presumed to be caused by reaction of fluids with limestone and to depend on the oxidation state [38]. Where the ratio of water to rock is high, the fluids can alter  $\delta^{13}\text{C}$  easier than  $\delta^{18}\text{O}$  during reaction with limestone, because the  $^{13}\text{C}$  contents of the fluids are negligible. The lowest values of  $\delta^{18}\text{O}$  in carbonates are mainly those of skarn calcite and dolomite (Type II).  $\delta^{18}\text{O}$  values of skarn calcite and dolomite are more similar to those of the Sarnowsar granite than to those of the fresh carbonates.  $\delta^{18}\text{O}$  values of the skarn calcite and dolomite fall in the middle of some subparallel curves, which connect the  $\delta^{18}\text{O}$  and  $\delta^{13}\text{C}$  values of marine carbonates and magmatic fluids (Figs. 5 and 6). The large isotopic shifts in  $\delta^{18}\text{O}$  and  $\delta^{13}\text{C}$  of calcite and dolomite from the Sangam deposits can only be explained by water-rock interaction between marine carbonates and magmatic fluids. [8] showed that the Sangam deposit is an igneous-metasomatic skarn resulting from an infiltration of hydrothermal fluids in the carbonate rocks. The calculated paths in Figure 7 show that a complete decarbonation could result in a large depletion in  $^{13}\text{C}$ , while the  $^{18}\text{O}$  depletion is negligible. In contrast, interaction of fluids with carbonates causes a large  $^{18}\text{O}$  depletion in marble at early stages, whereas  $^{13}\text{C}$  depletion for calcite and dolomite marbles is negligible. During the last stages where fluid/water ratio is very high,  $\delta^{18}\text{O}$  and  $\delta^{13}\text{C}$  values of calcite or dolomite are close to those of the

fluid. In these stages  $^{18}\text{O}$  depletions in carbonates remain almost constant, while  $^{13}\text{C}$  depletions are very large. Therefore, as water/rock ratio increases, depletion rate changes and  $^{13}\text{C}$  depletion becomes large for calcite and dolomite. This change in depletion type is believed to have resulted because progressively increasing water to rock ratio. There are models that can be used to describe the nature and the amounts of isotopic alteration of carbonate host rocks as a function of progressively increasing water to rock ratio in cases where temperature and  $X(\text{CO}_2)$  are known. Such approaches have been frequently applied to interpret variations of  $\delta^{18}\text{O}$  and  $\delta^{13}\text{C}$  values of carbonate rocks from contact aureoles and skarn deposits, for example by [12, 14, 23, 39, 44]. The following mass balance equation of [45] was used to model the isotopic changes of carbonate rocks in the Sangam deposit. For oxygen isotopic exchange, this is:

$$w/r = (\delta^{18}\text{O}_{\text{rock}}^f - \delta^{18}\text{O}_{\text{rock}}^i) / (\delta^{18}\text{O}_{\text{H}_2\text{O}} + \Delta - \delta^{18}\text{O}_{\text{rock}}^f)$$

Where  $\Delta$  is oxygen isotopic fractionation factor between mineral and water,  $i = \text{initial}$ ,  $f = \text{final}$ , rock is here calcite or dolomite and  $w/r$  is the atom mass ratio of water to rock. The isotopic fractionation factors were calculated using the following equations:  $\Delta_{\text{calcite-water}} = 2.78(10^6/T^2) - 2.89$  (Friedman and O'Neil, 1977) and  $\Delta_{\text{dolomite-water}} = 3.2(10^6/T^2) - 1.5$  [31]. Carbon isotopic exchange, in relation to the concentration of carbon in the fluid is similarly given by:

$$X_{\text{CO}_2} \times w/r = (\delta^{13}\text{C}_{\text{rock}}^f - \delta^{13}\text{C}_{\text{rock}}^i) / (\delta^{13}\text{C}_{\text{CO}_2} + \Delta - \delta^{13}\text{C}_{\text{rock}}^f)$$

Where  $\Delta$  is carbon fractionation factor between calcite or dolomite and  $\text{CO}_2$ ,  $X(\text{CO}_2)$  is mole fraction of  $\text{CO}_2$  in the fluid. The isotopic fractionation factors are calculated using the following equations:  $\Delta_{\text{calcite-CO}_2} = 2.988(10^6/T^2) - 7.666(1000/T) + 2.46$  and  $\Delta_{\text{dolomite-CO}_2} = 3.16(10^6/T^2) - 7.666(1000/T) + 2$  [17]. These equations describe a closed system where all of the fluid completely equilibrates with the rock and isotopic exchange is dependent on the temperature and fluid/rock ratio. Isotopic exchange of the fluids with surrounding rocks can also be modeled with an open system using the following equation by [45]:

$$w/r = \ln[(w/r)_{c-s} + 1]$$

where  $[(w/r)_{c-s}]$  is the value obtained from the closed system. This equation can be used for both O and C.

The  $\delta^{13}\text{C}$  values of some skarn calcite and dolomite in the studied area are as low as  $-7.5$  ‰, which is within the range those of carbonatites [50]. Therefore,  $\delta^{13}\text{C}$

value of fluid for the starting point is assumed  $-8.0$  for the calculations.  $\delta^{18}\text{O}$  value of the initial water is that in equilibrium with the Sarnowsar granitoid ( $+9.0$  ‰). The  $\delta^{18}\text{O}$  and  $\delta^{13}\text{C}$  value of calcite for the starting point is close to those of Khajeh Anjireh for calcic skarn zone and the value of fresher dolomite for magnesian skarn zone. The  $X(\text{CO}_2)$  is estimated from the mineral assemblages of the studied area.

The  $\delta^{18}\text{O}$ - $\delta^{13}\text{C}$  variation curve diagrams shown in Figure 8 are the result of mutual interaction between the hydrothermal solutions ( $\delta^{13}\text{C} = -8.0$  ‰ and  $\delta^{18}\text{O} = +9.0$  ‰) and the fresh limestone ( $\delta^{18}\text{O} = 20.0$  ‰,  $\delta^{13}\text{C} = 1.0$  ‰) at temperatures of  $500$  and  $300^\circ\text{C}$  in closed and open systems with  $X(\text{CO}_2) = 0.05$  and water/rock ratio of  $0$  to  $100$  % for calcite from the calcic skarn zone. The  $\delta^{18}\text{O}$  and  $\delta^{13}\text{C}$  values of skarn calcite from the calcic skarn zone do not fit well on the calculated  $\delta^{18}\text{O}$  and  $\delta^{13}\text{C}$  trends shown on Figure 8. Some data can be explained by the calculated curves at  $500^\circ\text{C}$  and water/rock ratio of up to  $20$  % in a closed system (Fig. 8). However, with a higher  $\delta^{13}\text{C}$  value of calcite for the starting point, data would adequately fit on the calculated  $\delta^{18}\text{O}$ - $\delta^{13}\text{C}$  variation curve diagrams at  $500^\circ\text{C}$  in both closed and open systems. Therefore, the low  $\delta^{18}\text{O}$ - $\delta^{13}\text{C}$  value of skarn calcite can be interpreted by infiltration of the magmatic water in the calcic skarn. The calculated curve at  $300^\circ\text{C}$  in the closed system and the calculated curves in the open system cannot explain the observed data. If the curves for the water-rock interaction are calculated at various conditions (for example, over a wide range of temperatures), a series of sub-parallel curves would result, which encompass the entire field of observed data for the calcite types. Therefore the amount of  $\delta^{18}\text{O}$  and  $\delta^{13}\text{C}$  is influenced by several factors, such as initial isotopic composition of rock and fluid, temperature, water-rock ratio and  $X(\text{CO}_2)$ . As Figure 8 shows the  $^{18}\text{O}$  and  $^{13}\text{C}$  depletion could mainly be explained with the curve of  $500^\circ\text{C}$  in a closed system. For this curve, the water-rock ratio is calculated to be less than  $5$  for calcite marble, about  $10$  for skarn calcites from magnetite-carbonate zone and magnesian zone, and about  $20$  for skarn calcite from garnet-magnetite zone. To explain these data in an open system, the temperature would have to be more than  $500^\circ\text{C}$ .

Similarly, the  $\delta^{18}\text{O}$ - $\delta^{13}\text{C}$  variation curves shown (Fig. 9) are the result of mutual interaction between the assumed hydrothermal solutions ( $\delta^{13}\text{C} = -8.0$  ‰ and  $\delta^{18}\text{O} = +9.0$  ‰) and wall rock dolomite ( $\delta^{18}\text{O} = 25.5$  ‰,  $\delta^{13}\text{C} = 0.0$  ‰) at temperatures of  $500^\circ$  and  $300^\circ\text{C}$  in closed and open systems with  $X(\text{CO}_2) = 0.01$  and water/rock ratio of  $0$  to  $100$  % for dolomite from the magnesian skarn zone. The  $\delta^{18}\text{O}$  and  $\delta^{13}\text{C}$  curves

derived from an open system do not adequately fit the  $\delta^{18}\text{O}$  and  $\delta^{13}\text{C}$  values of the carbonates from the magnesian skarn zone. However, the  $\delta^{18}\text{O}$  and  $\delta^{13}\text{C}$  values of the magnesian skarn zone can be mainly explained by the calculated curve at  $500^\circ\text{C}$  (Fig. 9). Even by assuming that  $\delta^{18}\text{O} = 6.0$  and  $3.0$  ‰ for hydrothermal solutions, the isotopic values of the

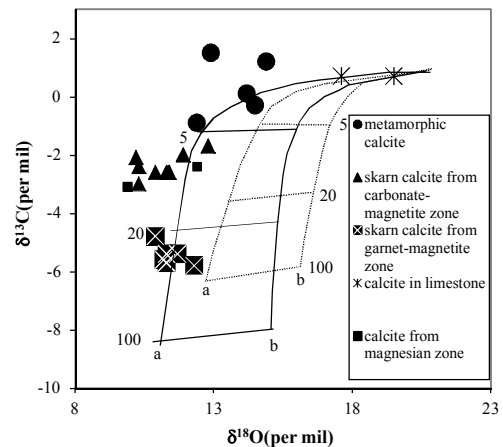


**Figure 8.** The isotopic mixing curves describe the variation in the oxygen and carbon isotope composition of calcite produced by interaction between water and limestone ( $\delta^{18}\text{O} = +20.0$  ‰ and  $\delta^{13}\text{C} = +1$  ‰) and a fluid ( $\delta^{18}\text{O} = +9.0$  ‰ and  $\delta^{13}\text{C} = -8.0$  ‰), at temperatures of  $500$  and  $300^\circ\text{C}$  for open (dashed lines) and closed (solid lines) systems. The curves are graduated in increments of W/R ratio.

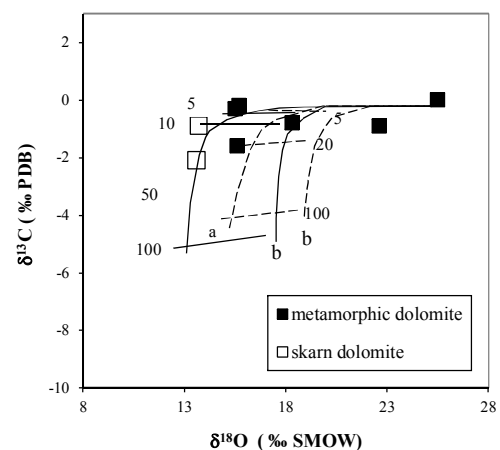


**Figure 9.** The isotopic mixing curves describe the variation in the oxygen and carbon isotope composition of calcite and dolomite produced by interaction between wall rock dolomite ( $\delta^{18}\text{O} = 25.5$  ‰ and  $\delta^{13}\text{C} = 0.0$  ‰) and a fluid ( $\delta^{18}\text{O} = +9.0$  ‰ and  $\delta^{13}\text{C} = -8.0$  ‰) at temperatures of  $500$  (a) and  $300^\circ\text{C}$  (b) for open (dashed lines) and closed (solid lines) systems. The curves are graduated in increments of W/R.

magnesian zone can be explained by the 300° C curve. Therefore, hydrothermal solutions that circulated in the magnesian skarn zone may be magmatic water partially mixed with externally derived water, for example local meteoric water.

The following points are conclusions: The high  $\delta^{18}\text{O}$  values of the I-type Sarnowsar granitoid and felsic dykes was mainly produced by sub-solidus processes, such as deuteric and (or) hydrothermal alteration; these fluids at relatively low temperatures slightly altered the isotopic composition shifting them to higher values.

Both simple Batch and Rayleigh decarbonation models are insufficient to explain the large isotopic shifts of the marble calcite and some of the dolomite marbles. Mineralized limestone is strongly altered in its isotopic composition relative to barren limestone of Khageh Anjireh.

A large decrease of  $\delta^{18}\text{O}$  and  $\delta^{13}\text{C}$  from metamorphic calcite toward skarn calcite among the skarn zones, and orebodies appear to be due an increase of infiltrative water/rock ratio.

High amounts of fluids can alter  $\delta^{13}\text{C}$  more than  $\delta^{18}\text{O}$  during reaction with limestone, because  $^{13}\text{C}$  contents of the fluids are negligible relative to limestone. The garnet-magnetite zone contains negligible limestone, therefore the fluids are dominant and both  $\delta^{18}\text{O}$  values and both  $\delta^{13}\text{C}$  values are those of magmatic water, whereas in the carbonate-magnetite zone and magnesian zone, high volume of marbles caused enrichment in  $\delta^{13}\text{C}$ .

The isotopic variations in the Sangan deposits can be well explained by mass balance calculation models. The  $\delta^{18}\text{O}$  and  $\delta^{13}\text{C}$  values of carbonates of type I and II from the calcic skarn zone are mainly explained by hydrothermal solutions ( $\delta^{13}\text{C} = -8.0\text{‰}$  and  $\delta^{18}\text{O} = +9.0\text{‰}$ ) interacting with fresh limestone ( $\delta^{18}\text{O} = 20.0\text{‰}$ ,  $\delta^{13}\text{C} = 1.0\text{‰}$ ) at 500°C with  $X(\text{CO}_2) = 0.02$  and water / rock ratio of up to 20. The  $\delta^{18}\text{O}$  and  $\delta^{13}\text{C}$  values of the magnesian skarn zone can be also explained by curved trends at 500° and  $\delta^{18}\text{O} = +9.0\text{‰}$ . Even by assuming that  $\delta^{18}\text{O} = +3.0\text{‰}$  for hydrothermal solution, the isotopic value of the magnesian zone are explained by a curved trend at 300°C.

### Acknowledgements

We thank the geologist and staff of the Sangan mine for providing the facilities and kindly helping us during our field study. The senior author would like to acknowledge the ministry of Education of Japan for the fellowship during his study at Akita University. This study was also supported by University of Sistan and Baluchestan to complete.

### References

1. Alavi, M. Tectonic of the Zagros orogenic belt of Iran: new data and interpretations. *Tectonophysics* **229**: 211-238 (1994).
2. Alavi Naini, M. Geological quadrangle map of Khaf: series sheet 8059, ministry of mines and metals. Geological survey of Iran, Tehran (1980).
3. Baumgartner, L. P. and Valley, J. W. Stable isotope transport and contact metamorphic fluid flow. *Rev. Mineral.* **40**: 415-467 (2001).
4. Berberian, M. and King, G. C. Towards a paleogeography and tectonic evolution of Iran. *Can. J. Earth Sci.* **18**: 210-265 (1981).
5. B.H.P.E. Sangan Iron project description. National Iran Steel Company (NISCO), Sangan, RE-0065 (1993).
6. Bodnar, R. G. and Vityk, M. O. Interpretation of microthermometric data for H<sub>2</sub>O-NaCl fluid inclusions. In: DeVivo B, Frezzotti, ML (eds) Fluid inclusions in minerals: methods and applications. IMA short course volume, Virginia Polytechnic Institute and State University Press: 117-130 (1994).
7. Boomeri, M. Genesis of the Sangan Iron ore, Northeast Iran. MS. thesis, Teacher Training University of Tehran: 270 p. (Persian) (1992).
8. Boomeri, M. Petrography and geochemistry of the Sangan iron skarn deposit and related igneous rocks, northeastern Iran. Ph.D. thesis, Akita University, Japan: 226 p (1998).
9. Boomeri, M., Mizuta, T., Nakashima, K., Ishiyama, D. and Ishikawa, Y. Geochemical characteristics of halogen-bearing hastingsite, scapolite and phlogopite from the Sangan iron skarn deposits, northeastern Iran. *J. Min. Pet. Econ. Geol.* **92**: 481-501 (1997).
10. Boomeri, M., Mizuta, T., Ishiyama, D., and Nakashima, K. Fluorine and chlorine in biotite from the Sarnowsar granitic rocks, northeastern Iran. *Iranian Journal of Science & Technology, Transaction A* **30**, **A1**: 111-125 (2006).
11. Bowman, J. R., O'Neil, J. R. and Essene, E. J. Contact skarn formation at Elkhorn, Montana. II: Origin and evolution of C-O-H skarn fluids. *Am. J. Sci.* **285**: 621-660 (1985a).
12. Bowman, J. R., Covert, J. J., Clark, A. H. and Mathieson, G. A. The Cantung E zone scheelite skarn orebody, Tungsten, Northwest Territories: Oxygen, hydrogen, and carbon isotope studies. *Econ. Geol.* **80**: 1872-1895 (1985b).
13. Bowman, J. R. Stable isotope systematics of skarns. In Lentz DR (ed) Mineralized intrusion-related skarn systems. Mineral Assoc Canada Short course series **26**: 99-146 (1998).
14. Brown, P. E., Bowman, J. R. and Kelly, W. C. Petrologic and stable isotope constraints on the source and evolution of skarn-forming fluids at Pine Creek, California. *Econ. Geol.* **80**: 72-95 (1985).
15. Einaudi, M.T. Meinert, L. D. and Newberry, R. j. Skarn deposits. *Econ. Geol.* 75 the Anniversary Volume: 317-391 (1981).
16. Franchini, M., B., Meinert, L. D. and Montenegro, T. F.. Skarns Related to Porphyry-Style Mineralization at Caicayén Hill, Neuquén, Argentina: Composition and

- Evolution of Hydrothermal Fluids. *Econ. Geol.* **95**: 1197-1214 (2000).
17. Friedman, I. and O'Neil J. R. Compilation of stable isotopic fractionation factors of geochemical interest. *U.S. Geol. Surv. Prof. Pap.*: 440-KK (1977).
  18. Haruna, M. and Ohmoto, H. Oxygen and carbon Isotope studies on the skarn type ores at the Tengumori copper deposit of the Kamaishi mine, northeastern Japan. *Resource Geol.* **46**: 125-136 (1996).
  19. Hezarkhani, A. and Williams-Jones, A., E. Controls of alteration and mineralization in the Sungun porphyry copper deposit, Iran: Evidence from fluid inclusions and stable isotopes. *Econ. Geol.* **93**: 651-670 (1998).
  20. Karimpour, M. Investigation on origin and formation mechanism of Sangan iron ore deposit. Khorassan, Iran. *Iron ore Symposium, National Iran Steel* (1990).
  21. Kermani, A. and Forster, H. Petrography, Mineralogical and geochemical investigations of the Sangan Iron ore deposit, northeastern Iran. *Proceedings of third mining symposium of Iran* (1991).
  22. Kita, I. and Matsubaya, O. F<sub>2</sub> technique for the oxygen isotopic analysis of silica minerals. *Rep. Res. Inst. Nat resour. Min. coll. Akita Univ.* **48**: 25-33 (1983).
  23. Layne, G. D., Longstaffe, F. J., and Spooner, E. T. C. The JC Tin skarn deposit, southern Yukon Territory, II: A carbon, oxygen, hydrogen and sulfur stable isotope study. *Econ. Geol.* **86**: 48-65 (1991).
  24. Mazaheri, S. A. Petrological studies of skarns from Marulan South, New South Wales, Australia and Sangan, Khorasan, Iran. Ph.D. thesis, University of Wollongong, New South Wales, Australia (1995).
  25. McCrea, J. M. On the isotopic chemistry of carbonates and a paleotemperature scale. *J. Chem. Phys.* **18**: 849-857 (1950).
  26. Meinert, L. D. Skarn manto and breccia Pipe formation in sedimentary rocks of the Cananea Mining district, Sonora Mexico, *Econ. Geol.* **77**: 919-949 (1982).
  27. Meinert, L. D., Lentz, D. R. and Newberry, R. J. Introduction, *Econ. Geol.* **95**: 1183-1184 (2000).
  28. Morishita, Y. Three-dimensional isotopic characteristics of crystalline limestone around the Sakonishi Zn ore bodies in the Kamioka mining district, Japan. *Resource Geol.* **49**: 243-257 (1999).
  29. Murakami, H. and Nakano, T. Hydrothermal alteration of limestone and mineral exploration of Zn-Pb skarn deposits in the Sako-nishi area of the Kamioka mine, central Japan. *Resource Geol.* **49**: 259-280 (1999).
  30. Nabelek, P. I., Labotka, T. C., O'Neil, J. R., Papike, J. J. Contrasting fluid/rock interaction between the Notch Peak granitic intrusion and argillites and limestones in western Utah: evidence from stable isotopes and phase assemblages. *Contributions to Mineralogy and Petrology* **86**: 25-34 (1984).
  31. Northrop, D. A. and Clayton, R. N. Oxygen-isotope fractionation in systems containing dolomite. *Jour., Geol.* **74**: 174-196 (1966).
  32. O'Neil, J. R. and Taylor, H. P. Jr. The oxygen isotope and cation exchange chemistry of feldspars. *American Mineralogist* **52**: 1414-1437 (1967).
  33. Richards, I. J., Labotka, T. C., and Gregory, R. T. Contrasting stable isotope behavior between calcite and dolomite marbles, Lone Mountain, Nevada. *Contr. Mineral. Petrol.* **133**: 202-221 (1996).
  34. Roedder, E. Fluid inclusions. *Rev. Mineral.* **12**: 413-471 (1984).
  35. Rose, A. W., Herrick, D. C., and Deines, P. An oxygen and sulfur isotope study of skarn-type magnetite deposits of the Cornwall type, southeastern Pennsylvania. *Econ. Geol.* **80**: 418-443 (1985).
  36. Shieh, Y. N., Taylor, H.P. Jr. Oxygen and carbon isotope studies of contact metamorphism of carbonate rocks. *Journal of Petrology* **10**: 307-331 (1969).
  37. Sheppard, S. M. F. and Schwacz, H. P. Fractionation of carbon and oxygen isotopes and magnesium between coexisting metamorphic calcite and dolomite. *Contr. Mineral. Petrol.* **26**: 161-198 (1970).
  38. Shimazaki, H., Shimizu, M. and Nakano, T. Carbon and oxygen isotopes of calcites from Japanese skarn deposits. *Geochem. J.* **20**: 297-310 (1986).
  39. Shin, D. and; Lee, I. Carbonate-hosted talc deposits in the contact aureole of an igneous intrusion (Hwanggangri mineralized zone, South Korea): geochemistry, phase relationships, and stable isotope studies. *Ore Geology Review.* **22**: 17-39 (2003).
  40. Stocklin, J. Structural history and tectonics of Iran, a review. *American Association of Petroleum Geologists Bulletin* **52**(7): 1229-1258 (1968).
  41. Streckeisen, A. L., Classification and nomenclature of plutonic rocks; recommendations. *Geotimes*, **18**: 10, 26-30 (1973).
  42. Sverjensky, D. A. Isotopic alteration of carbonate host rocks as a function of water to rock ratio-An example from the Upper Mississippi valley zinc-lead district. *Econ. Geol.* **76**: 154-172 (1981).
  43. Taylor, B. E and O'Neil, J. R. Stable studies of metasomatic Ca-Fe-Al -Si skarns and associated metamorphic and igneous rocks, Osgood Mountains, Nevada. *Contr. Mineral. Petrol.* **63**: 1-50 (1977).
  44. Taylor, B. E and Nurminen, K. B. Oxygen and carbon isotope and cation geochemistry of metasomatic carbonates and fluids, Bergell aureole, northern Italy. *Geochim. et cosmochim. Acta* **50**: 1267-1279 (1986).
  45. Taylor, H.P. Jr. Water / rock interactions and the origin of H<sub>2</sub>O in granitic batholiths. *J. Geo. Soc. Lond.* **133**: 509-559 (1977).
  46. Taylor, H.P. Jr., Oxygen and hydrogen isotope studies of plutonic granitic rocks. *Earth Planet, Sci. letters* **38**: 177-210 (1978).
  47. Taylor, H.P. Jr. and Sheppard, S. M. F. Igneous rocks: I. Processes of isotopic fractionation and isotope systematics. *Rev. Mineral.* **16**: 227-271 (1986).
  48. Ternet, Y. Explanatory text of the Taybad quadrangle map 1/250000. Ministry of mines and metals, geological survey of Iran, Tehran: 200 p (1990).
  49. Tornos, F. and Spiro, B. F. The Geology and Isotope Geochemistry of the Talc Deposits of Puebla de Lillo, (Cantabrian Zone, Northern Spain) *Econ. Geol.* **95**: 1277-1296 (2000).
  50. Valley, J.W. Stable isotope geochemistry of metamorphic rocks, *Rev. Mineral.* **16**: 445-489 (1986).
  51. Walker, R. and Jackson, J., Offset and evolution of the Gowk fault, S.E, Iran: a major intra-continental strike-slip system, *Journal of Structural Geology* **24**: 1677-1698 (2002).
  52. Zaw, K. and Singoyi, B. Formation of Magnetite-Scheelite Skarn Mineralization at Kara, Northwestern Tasmania: Evidence from Mineral Chemistry and Stable Isotopes. *Econ. Geol.* **95**: 1215-1230 (2000).